VIA MEDICA

Nuclear Medicine Review 2004
Vol. 7, No. 1, pp. 7–12

ISSN 1506–9680

Original

Prediction of left ventricular ejection fraction in patients with coronary artery disease based on an analysis of perfusion patterns at rest. Assessment by an artificial neural network

Bogusław Stefaniak, Witold Cholewiński, Anna Tarkowska

Chair and Department of Nuclear Medicine, Skubiszewski Medical University of Lublin, Poland

[Received 13 IV 2004; Accepted 26 IV 2004]

Abstract

BACKGROUND: In CAD, left ventricular function depends on the condition of myocardial perfusion, hence it may be presumed that blood flow abnormalities may enable the LVEF to be predicted. The aim of the study was to apply an Artificial Neural Network (ANN) to investigate the relationships between myocardial perfusion and LVEF, measured simultaneously.
MATERIAL AND METHODS: gSPECT examinations were performed in 95 patients with CAD, divided into training (n = 50) and testing (n = 45) groups. using the acquired data, in each subject the LVEF was calculated and a perfusion polar map was constructed and divided into 25 segments. Based on results obtained in the training group, a characteristic configuration of segments was defined, with features enabling differentiation between the individual subjects of that group. The set of those segments, as well as the corresponding LVEF values enabled the optimum network architecture to be constructed and trained. The trained ANN was verified by application to the testing group.
RESULTS: Using the above-described procedure, 15 polar map segments were defined which enabled the patients of the training group to be differentiated sufficiently enough to make their further recognition possible. The optimal network structure consisting 25 neurons was obtained by comparing the activity in those segments in individual subjects with corresponding LVEF values. Based on the above model, the obtained network was able to reproduce learning data (r = 0.832; learning error = = 4.84%) and to apply the gained knowledge to the testing cases (r = 0.786; testing error = 4.99%).
CONCLUSIONS: The obtained network can generalise learned information. To predict LVEF, some polar map segments should be excluded from the analysis. Erroneous LVEF prediction may occur resulting mainly from conditions independent from perfusion abnormalities.
Key words: myocardial perfusion, polar map, LVEF, artificial neural networks

Correspondence to: Boguslaw Stefaniak
Chair and Department of Nuclear Medicine
Skubiszewski Medical University of Lublin
ul. Jaczewskiego 8, 20–954 Lublin, Poland
Tel: (+48 81) 72 44 339, e-mail: ziemowit@asklepios.am.lublin.pl

Introduction

Transformation of the data acquired by the myocardial single-photon emission computed tomography (SPECT) into a polar map is a common procedure used to assess semiquantitatively distribution of perfusion within the heart muscle [1, 2]. Thanks to the circular form and standard dimensions, the polar map image is independent from the individual shape and size of the left ventricle. This enables the reference (normal) perfusion distribution to be defined from the data obtained in a group of healthy subjects. By comparing a patient's polar map image with the normal perfusion distribution, regional abnormalities can be detected,

Nuclear Medicine Review 2004, Vol. 7, No. 1

localised and quantified [2]. Parametric images generated to present those abnormalities, supplemented with various numerical indices have been shown to be of great value in assessing the intensity and extent of blood flow changes in patients with coronary artery disease (CAD), as well as in prognosis and follow-up [2, 3].

It has been proven that in CAD, local deterioration of myocardial perfusion may lead to regional contraction abnormalities and to an impairment of left ventricular global function, with an left ventricular ejection fraction (LVEF) decrease. Based on these observations, it seems justified to presume that it would be possible to predict the LVEF from the blood flow pattern.

The introduction of gSPECT technique [4] made it possible for myocardial perfusion and left ventricular function to be assessed simultaneously, yielding LVEF values comparable to those obtained with other methods, such as a gated blood pool study first of all. Such simultaneous evaluations of the left ventricular perfusion and function, based on the same data acquired during activity measurements, enables a direct comparison to be made between these two parameters, and, consequently, a determination of the relationships between them.

However, because of this comparison some problems connected with the data analysis should be taken into account. Such a rudimentary method as the linear regression analysis can hardly be considered adequate for comparing the great number of input variables obtained from all polar map segments with the LVEF values. Various other methods used in the data processing also do not meet all necessary requirements, essential for this comparison to be made.

In several papers it has been shown that artificial intelligence, which is commonly known to be a flexible scientific tool, may be useful in the interpretation of myocardial perfusion polar maps and in defining relationships between data presented in those images and various other physiopathological phenomena [5]. Among others, ANNs have been applied successfully to compare regional radionuclide distribution patterns in myocardium in patients with CAD with the intensity, extent and localisation of coronary artery changes. Based on those results it may be expected that this method would be suitable for a comparison between perfusion distribution as presented in the polar map and the LVEF. To our knowledge, such a study has not been performed yet.

In fact, artificial neural networks, usually simulated by the computer, have become a separate branch of knowledge. As a result of earlier investigations, various ANNs algorithms ready for use have been obtained and applied to several computer platforms. Hence, it can be considered justified to employ these algorithms to evaluate relationships between the myocardial perfusion patterns and the left ventricular (LV) global function and to predict the LVEF value, based on the blood flow distribution.

The aim of this study was to apply ANN to investigate relationships between the distribution of perfusion as presented in polar map images obtained from gSPECT at rest, and the LVEF calculated from the same acquisition data.

Material and methods

Ninety-five patients with angiographically confirmed CAD underwent a myocardial gSPECT 1 hour after an intravenous injection of 740 MBq ^{99m}Tc-tetrofosmin at rest. Examinations were performed using a double-headed, large field of view gamma camera (Varicam, GE Medical Systems) connected to a dedicated computer (Xpert, GE Medical Systems). Both of the detectors were equipped with low energy, high resolution, parallel hole collimators and positioned at an angle of 90° in relation to each other. Data were acquired in 60 projections, 50 sec. each, by both detectors jointly (30 projections by each of them) in step-and-shoot mode over a 180° circular orbit modified by body contouring, from the 45° RAO to the 45° LPO view. The activity was measured using gated technique, with the cardiac cycle divided into 8 sequences. A 20% symmetric energy window, centred on the 140 keV peak was used. Data were acquired with a zoom factor of 1.28 and stored in a 64×64 computer matrix. A tomographic reconstruction was performed by means of a filtered back projection, using a Butherworth filter with an order of 5.0 and a cut-off frequency of 0.30 cycles/pixel. Attenuation and scatter corrections were not performed. In each case the LVEF was calculated by the method of Germano et al. using dedicated software. To assess myocardial perfusion semi quantitatively, polar maps were constructed from gSPECT data converted into a non-gated study and were divided into 25 segments. In each segment the average cts/pixel number was calculated and expressed as a percentage of the cts/pixel value in the segment with the maximum activity. For ANN data evaluation, the clinical material was divided randomly into the training group ($n = 50$; 14 females, 36 males; average age 55.3 years) and the testing group ($n = 45$; 21 females, 24 males; average age 55.4 years). Artificial neural network was simulated on a PC computer using commercial software STATISTICA StatSoft, Inc.v.6. for Microsoft Windows. The network with radial basis functions was selected as an optimal ANN type for comparing empirical data obtained from segmental activities with the LVEF. The sets of 25 polar map values and corresponding LVEF values found in the training group were used to indicate segments with activity patterns optimal for clear-cut identification of any subject in that group and for differentiating that subject from the other cases. These segments were indicated by the program automatically, based on a balanced network performance (minimum errors of prediction in training and testing groups) as well as on the variety of network structure and on the configuration of used input variables. For this purpose, the program calculated the prediction error quotient for each variable using sensitivity analysis. This quotient was expressed as the relation between the prediction error found for the model with a removed given input variable and the total network error calculated based on all variables. The above-indicated segments enabled the construction of an optimal network architecture and its training.

The Network was learned using a 2-fold cross-validation scheme. Centres of radial basal functions were created randomly from the training group, using Kohonen's method. The radii of the basal function were equal to 1.

Verification of trained ANN was done by its application to the testing group and by comparing the predicted LVEFs with the measured ones in both groups. The obtained results were subjected to statistical analysis, including the two-way joining method applied to the assessment of the feature grouping.

Results

One or more perfusion defects were found at rest in 88 subjects (46 cases in the training group and 42 cases in the testing group). In the remaining 7 patients i.e. in 4 training subjects and 3 testing ones, no perfusion abnormality was detected.

Left ventricular ejection fraction values ranged in the total material from 15% to 75% (mean 49.8%), in the training group from 17% to 75% (mean 51.5%) and in the testing group from 15% to 70% (mean 48.2%). The average LVEF in the testing group did not differ significantly from that in the training group ($p > 0.05$).

Statistical analysis (two-way joining), applied to the spatial arrangement of characteristic polar map activity features and to the corresponding alignment of individual cases in the total clinical material, revealed several clustered perfusion patterns, presented in Figure 1 as activity distribution variations along the vertical axis.

These clusters were shown on the polar map images in accordance with the location of 4 arbitrarily selected areas defined according to the arrangement of the regions involved and in agreement with the anatomical subdivision of the LV myocardium. They consisted of 3–11 segments, presented in Figure 1 as grey coloured parts of polar map diagrams localised below the horizontal axis (C).

The results obtained by the neural net in the training group using the program procedures described in the chapter "Material and methods", revealed a characteristic configuration of 15 segments, which enabled individual subjects in this group to be differentiated from each other (Fig. 2 — grey coloured segments).

Those segments were scored according to their error, from that one with the lowest error contribution (E = 1.272; segment No. 22) through those with a progressively ascending error contribution (segments no. 12, 18, 5, 15, 8, 1, 11, 13, 6, 4, 17, 10, 16) to that with the highest error contribution (E = 0.998; segment No. 9).

The optimal network structure, obtained by comparing activity in the above segments of individual subjects with corresponding LVEF values, consisted of 36 neurons and 320 connections between them (Fig. 3). This structure included 15 input neurons, a set of 20 neurons in the hidden layer and 1 output neuron.

A statistical analysis revealed that the above network was able to reproduce learning data with a learning error of 4.84%. A good agreement was found between the LVEF values measured by gSPECT and those predicted using the obtained ANN model, with a correlation coefficient $r = 0.832$ ($p < 0.0001$); and a linear relation equation $Y = 0.795{*}X + 17.125$. Application of this ANN model to the testing cases showed similar results (testing error: 4.99%; $r = 0.786$; $Y = 0.827{*}X + 11.411$). The results of the replication of

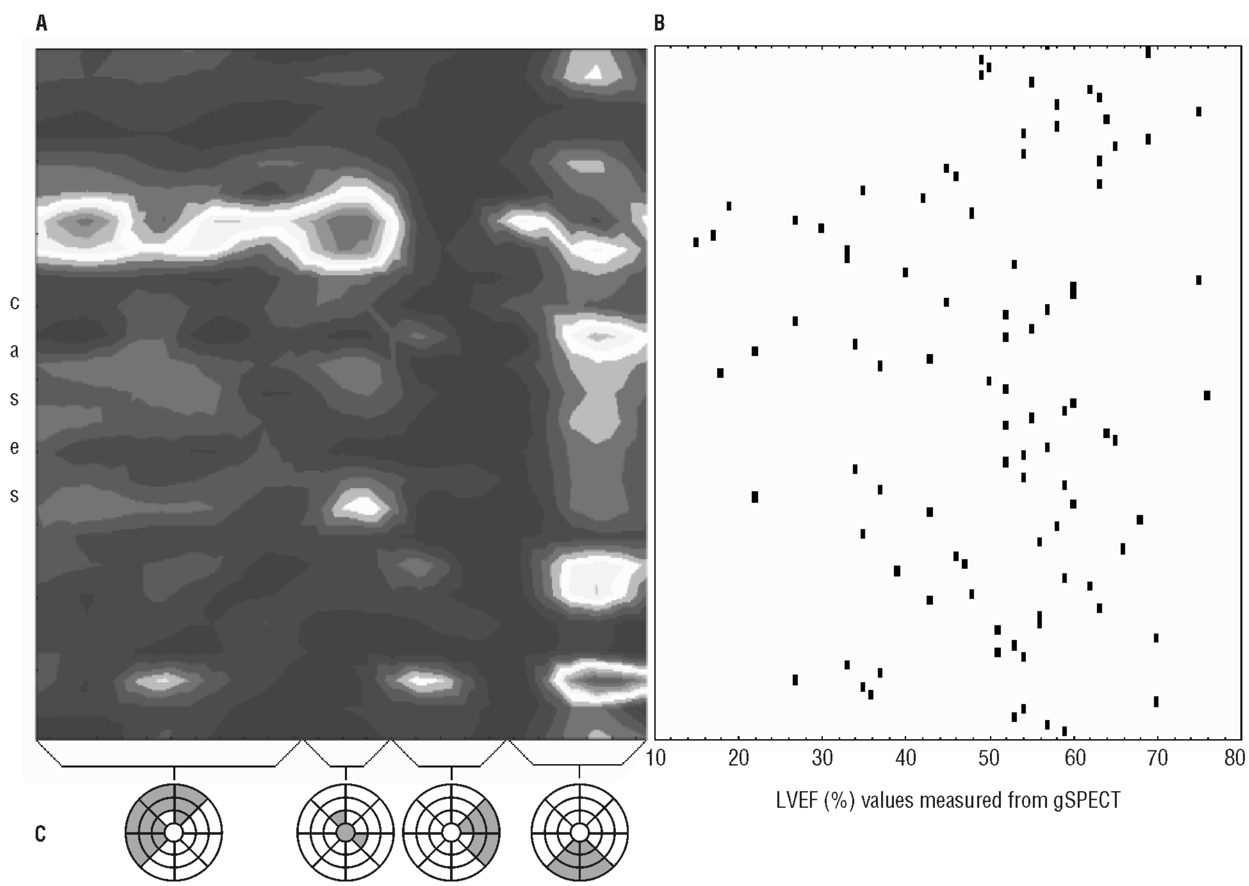

Figure 1. Results of two-way joining analysis (**A**) and LVEF values observed in individual subjects of the total group under study (**B**), in relation to the involved segments (grey coloured) (**C**). Part A contains 2375 numerical values obtained from 25 segments belonging to each of the 95 patients of both group. Values from each case were presented in grey scale, on a single row of the chart. Patient's order along the vertical axis was created by a two-way joining analysis, based on similarity of the activity patterns between adjacent cases and segments. Part C contains information about configuration of the segments within the polar map. Part B of the figure presents LVEF values observed in corresponding cases.

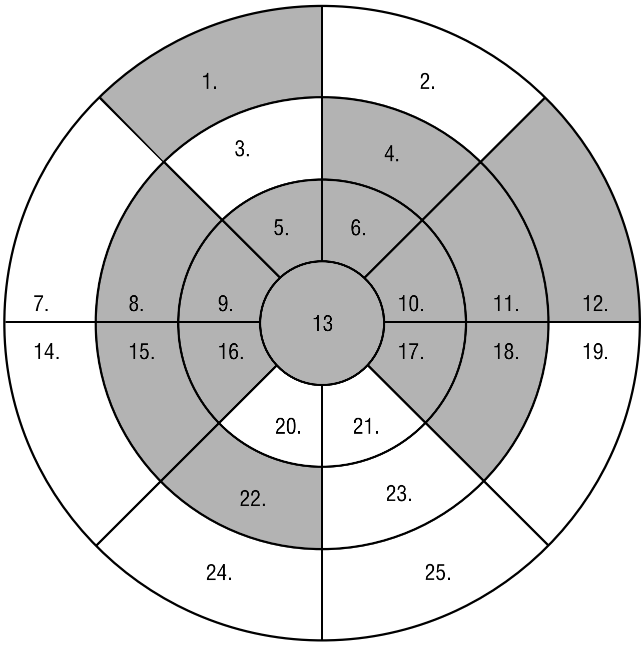

Figure 2. Perfusion polar map divided into 25 segments. Fifteen segments automatically selected to provide data for ANN inputs are grey coloured.

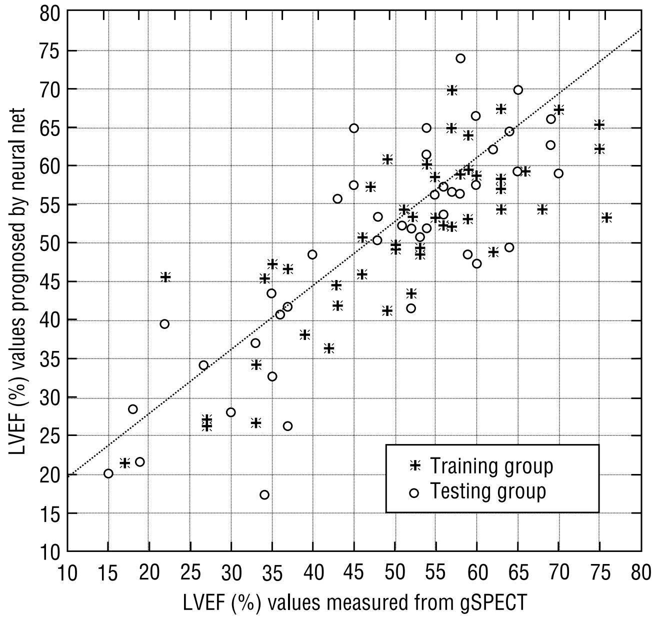

Figure 4. Relationship between LVEF values measured directly from gSPECT and LVEF values replicated by ANN in the training group and prognosticated in the testing group.

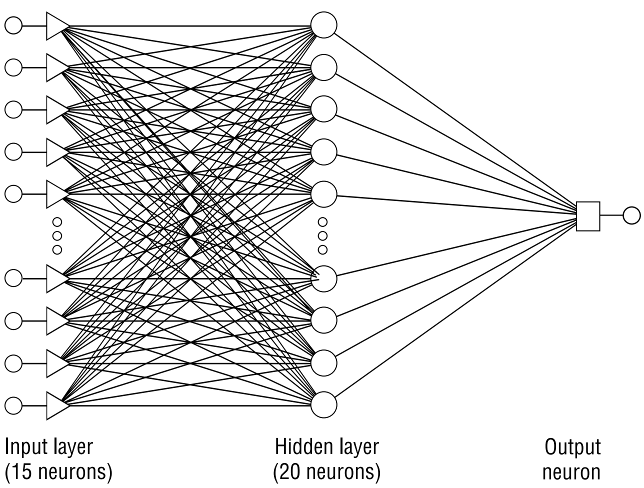

Figure 3. Network architecture selected automatically to evaluate relationships between perfusion patterns and ejection fractions.

the LVEF in the learning group and of LVEF prediction in the testing group are presented in Figure. 4.

Discussion

Nuclear medicine diagnosis involves processes of collection, analysis, recognition and classification of data stored in digital form [6]. For this purpose various methods are available, some of them yielding quantitative results. Among the quantitative procedures ANNs seem to be of special value because they can learn by example and not by the strict mathematical rules which are scarcely able to define abnormalities on medical images. The most important ANN feature, often used as case-based reasoning systems [2], is its possibility to produce correct outputs when the network is presented with input data-set not previously seen. This ability is called "generalisation" [6]. Until now the successful applications of ANNs in nuclear medicine have been most frequently focused on pulmonary embolism [7–12], and on myocardial [5, 13, 14] and brain perfusion [15, 16]. However, ANNs have not been applied to study relationships between left ventricular perfusion and function yet.

Page et al. [15] and Khorsand et al. [2] have reported that neural networks perform the classification tasks better than the other typical statistical methods. On the other hand, several other authors solving various medical problems observed with ANN a similar level of accuracy to that of logistic regression [17, 18]. However, such a simple method as regression analysis cannot be applied instead of ANN because its is not able to store a number of different patterns in a single equation. In our study, a typical statistical analysis (two-way joining) performed in the total clinical material showed in only several cases, a slight tendency to cluster similar perfusion patterns with nearly equal LVEF values together. Such results may confirm similarities between blood flow patterns but do not enable one to evaluate the LVEF directly, i.e. from the obtained graph.

All of the above characteristic features of ANNs fully justify the application of artificial intelligence to study relationships between myocardial perfusion patterns and LVEF.

In examinations of heart scintigrams with ANNs, the majority of authors divided original or processed cardiac image into various subregions, thus reducing the number of input variables. In the examples of this procedure as presented in some publications, perfusion polar maps were divided into various numbers of segments, up to as many as 256 [19].

Contrary to the above procedures, an interesting method not connected with the defining anatomical ROI's was reported by Levy for the evaluation of brain and by Lindahl for heart examination [20, 21]. This method was based on the two-dimensional Fourier Transform analysis. Unfortunately, the obtained number of up to 72 Fourier frequency components may be greater than or equal to the number of typical elements resulting from LV polar map subdivision [20].

Both of the above-mentioned ANN approaches performed either with or without scintigraphic image subdivision, may be used for the detection and localization of abnormalities present in the whole investigated area.

As regards pattern recognition, the great number of input data including such as, for example, all pixels describing empirically a phenomenon under study, may introduce non-significant or redundant information, therefore decreasing overall accuracy [20]. However, usually no mathematical selection of input variables was performed prior to their assessment by ANN. To overcome problems of redundant data, constructors of the ANN software had implemented a "sensitivity analysis" procedure eliminating superfluous variables and leaving only those which were necessary to preserve relevant information.

In this study, the sensitivity analysis indicated 15 segments which extracted characteristic features of training cases enabling the LVEF to be evaluated from the polar maps. This reduction of input variables favourably increased the ratio between the number of learning cases and the number of network inputs from 50:25 to 50:15. The structure and the number of connections within the whole network were determined, among other things, by the number of input variables. In our study, the number of the above connections is equal to 320. Gurney [22] indicated that the total number of training patterns should be at least 10 times greater than the number of connections in the network, but in a polemic article Boone [23, 24] emphasised that in the radiology practice this criterion is both unjustified and impossible to fulfil. Moreover, in studies by other authors the numbers of learning cases amounted to 45–1087 [12, 25]. In our material the numbers of learning and testing cases were similar to each other, which was in agreement with the data presented by some other authors [10, 23]. However, in some publications those numbers differ, usually with the learning group more numerous than the testing one [12, 19].

In this study, the amounts of learning (50 patients) and testing (45 patients) data sets were proved to be sufficient by the relatively low errors and good correlation between prognosticated and observed parameters.

The sensitivity analysis performed in our study showed that 15/25 automatically defined segments covered mainly territories supplied by LCX and LAD and to a smaller extent — that by RCA. As it was shown on Figure 1, the location of the majority of abnormal activity patterns revealed by a two-way joining analysis (part A, right-hand side) corresponded to the RCA territory on the polar map images (part C). The frequent location of activity defects in the RCA territory probably results from the known effect of radiation attenuation in the diaphragm. It may be presumed that such an activity distribution pattern was responsible for the frequent segment rejection within this region. The above arrangement of the segments defined by the sensitivity analysis, showed that the image features most important for the LVEF prediction were concentrated in the central part of the polar map. They were distributed homogeneously within the LCX territory, slightly dispersed within area supplied by LAD and occurring in only few segments within the RCA territory. Moreover, only two basal segments were included.

So far, feed-forward multilayer perceptrons (MLP) are the most frequent network algorithms used for the evaluation of images in nuclear medicine [5, 9, 10, 17]. Another network type with radial basis function (RBF) has also found wide-ranging applications in medical science [26, 27]. In comparison with other ANN types, the last of the two above-mentioned networks is characterised by a good ability to model experimental data, a simple structure with a singular hidden layer and a very short training phase. Such configuration of perceptrons containing one hidden layer was also a common architecture in previous applications of ANNs in nuclear medicine [12, 13, 19, 21, 28], which were used mainly for data classification [6].

The first application of the artificial network to patients with chest pain and suspected myocardial infarction was reported in 1989 [29]. It was a non-image application of artificial intelligence, trained on 174 subjects according to standard criteria used to classify low, medium and high cardiac risk patients.

Recently, applications of ANNs to heart diseases have been concentrated on detection, identification and scoring severity of LV regional perfusion abnormalities, using data obtained from SPECT rest/stress polar maps or, as earlier, from planar projections [27]. The results of the above-described examinations with ANNs have been presented in numerical format ranging from 0 to 1 with probabilistic interpretation of the output [7, 12, 13, 21]. The abnormalities were detected if the output data exceeded assumed threshold values calculated using operating characteristic curve analysis [12, 20].

The identification of these perfusion defects concerned the recognition of the involved LV territory. For the purpose of such identification, Lindahl et al. applied two different networks: the first of them for LAD and the second one for the RCA/LCX area [13].

Human perception is able to evaluate the severity and extent of activity defects on myocardial perfusion polar map images relatively easily but is not able to memorise a huge set of activity patterns and associated quantitative values. In this paper, the ANN algorithm revealed quantitative relations between myocardial perfusion patterns and LVEF. This finding suggests that in most cases such a relationship occurs in a typical, classified and anticipated manner. However, although in the total testing group a significant correlation was found between perfusion distribution and LVEF, in some cases the obtained results were of rather moderate correctness. Various mechanisms may be responsible for this phenomenon. Among other things, a peculiar character of image conversion to the polar map should be taken into account, which causes of information about shape and linear dimensions of the reconstructed object to be lost. Due to this effect, the resemblance between two polar maps may lead to the similar LVEF values generated on the net output, despite differences in the LV enlargement and resulting differences in the observed LVEFs. Another possible mechanism may be connected with errors resulting from incorrect localisation of the LV apex and basis areas based on arbitrarily accepted criteria.

In this paper, the interrelationship between observed and prognosticated LVEF values was slightly closer in the training group than in the testing one. It seems probable that the observed differences between correlation coefficients result mainly from the specific features of ANN analysis of biological phenomena, as well as from total errors which arose during the training of the model and its application. The automatic construction of the net architecture may also contribute to the relations between the above coefficients.

The developed algorithm for LVEF assessment based on a perfusion pattern is not intended to substitute this parameter measured by a gated SPECT, because the reported ANN method gives only a prediction. However, the presented method may be of significant value in the evaluation of LVEF when a gating procedure cannot be performed, in pts with arrhythmia first of all.

Unfortunately, the application of the above method to stress SPECT studies would be hardly possible because perfusion dependent activity distribution becomes fixed during exercise and LVEF measurements are performed 15–60 min. after stress, i.e. under rest conditions. Besides, a long lasting effect of physical stress may occur resulting in a decreased LVEF value [30].

Conclusions

The obtained network can generalise learned information. However, to predict the LVEF, some polar map segments should be excluded from the analysis. Erroneous LVEF prediction may occur resulting mainly from conditions independent from perfusion abnormalities.

References

1. Garcia EV, Van Train K, Maddahi J, Prigent F, Friedman J, Areeda A, Waxman A, Berman DS. Quantification of rotational Thallium-201 myocardial tomography. J Nucl Med 1985; 26: 17–26.
2. Khorsand A, Haddad M, Graf S, Moertl D, Sochor H, Porenta G. Automated assessment of dipyridamole ^{201}Tl myocardial SPECT perfusion scintigraphy by case-based reasoning. J Nucl Med 2001; 42: 189––193.
3. Lindahl D, Palmer J, Pettersson J, White T, Lundin A, Edenbrandt L. Scintigraphic diagnosis of coronary artery disease: myocardial bull's-eye images contain the important information. Clin Physiol 1998; 18: 554–561.
4. Germano G, Kiat H, Kavanagh PB, Moriel M, Mazzanti M, Su H-T, Van Train KF, Berman DS. Automatic quantification of ejection fraction from gated myocardial perfusion SPECT. J Nucl Med 1995; 36: 2138–2147.
5. Haraldsson H, Ohlsson M, Edenbrandt L. Value of exercise data for the interpretation of myocardial perfusion SPECT. J Nucl Cardiol 2002; 9: 169–173.
6. Scott R. Artificial intelligence: its use in medical diagnosis. J Nucl Med 1993; 34: 510–514.
7. Tourassi GD, Floyd CE, Coleman RE. Acute pulmonary embolism: cost-effectiveness analysis of the effectiveness analysis of the effect of artificial neural networks on patient care. Radiology 1998; 206: 81–88.
8. Scott JA, Palmer EL. Neural network analysis of ventilation-perfusion lung scans. Radiology 1993; 186: 661–664.
9. Holst H, Äström K, Järund A, Palmer J, Heyden A, Kahl F, Tägil K, Evander E, Sparr G, Edenbrandt L. Automated interpretation of ventilation-perfusion lung scintigrams for the diagnosis of pulmonary embolism using artificial neural networks. Eur J Nucl Med 2000; 27: 400–406.
10. Tourassi GD, Floyd CE, Sostman HD, Coleman RE. Acute pulmonary embolism: artificial neural network approach for diagnosis. Radiology 1993; 189: 555–558.
11. Tourassi GD, Floyd CE, Sostman HD, Coleman RE. Artificial neural network for diagnosis of acute pulmonary embolism: Effect of case and observer selection. Radiology 1995; 194: 889–893.
12. Evander E, Holst H, Järund A, Ohlsson M, Wollmer P, Äström K, Edenbrandt L. Role of ventilation scintigraphy in diagnosis of acute pulmonary embolism: an evaluation using artificial neural networks. Eur J Nucl Med Mol Imag 2003; 30: 961–965.
13. Lindahl D, Lanke J, Lundin A, Palmer J, Edenbrandt L. Improved classifications of myocardial bull's-eye scintigrams with computer-based decision support system. J Nucl Med 1999; 40: 96–101.
14. Hamilton D, Riley PJ, Miola UJ, Amro AA. A feed forward neural network for classification of bull's-eye myocardial perfusion images. Eur J Nucl Med 1995; 22: 108–115.
15. Page MPA, Howard RJ, O'Brien JT, Buxton-Thomas MS, Pickering AD. Use of neural networks in brain SPECT to diagnose Alzheimer's disease. J Nucl Med 1996; 37: 195–200.
16. Chan KH, Johnson KA, Becker JA, Satilin A, Mendelson J, Garada B, Holman BL. A neural network classifier for cerbal perfusion imaging. J Nucl Med 1994; 35: 771–774.
17. Cross SS, Harrison RF, Lee Kennedy R. Introduction to neural networks. Lancet 1995; 346: 1075–1079.
18. Baxt WG. Application of artificial neural networks to clinical medicine. Lancet 1995; 346: 1135–1138.
19. Fuita H, Katafuchi T, Uchara T, Nishimura T. Application of artificial neural network to computer-aided diagnosis of coronary artery disease in myocardial SPECT bull's-eye images. J Nucl Med 1992; 33: 272–276.
20. Levy AV, Gomez-Mont F, Volkow ND, Corona JF, Brodie JD, Cancro R. Spatial low frequency pattern analysis in positron emission tomography: a study between normals and schizophrenics. J Nucl Med 1991; 33: 287–295.
21. Lindahl D, Palmer J, Ohlsson M, Peterson C, Lundin A, Edenbrandt L. Automated interpretation of myocardial SPECT perfusion images using artificial neural networks. J Nucl Med 1997; 38: 1870–1875.
22. Gurney JW. Neural networks at the crossroads: caution ahead. Radiology 1994; 193: 27–28.
23. Boone JM. Sidetracked at the crossroads Radiology 1994; 193: 28–30.
24. Boone JM. Neural network at the crossroads. Radiology 1993; 189: 357–359.
25. Asada N, Doi K, MacMahon H, Montner SM, Giger ML, Abe C, Wu Y. Potential usefulness of an artificial neural network for differential diagnosis of interstitial lung diseases: pilot study. Radiology 1990; 177: 857–860.
26. Folland R, Hines EL, Boilot P, Morgan D. Classifying coronary dysfunction using neural networks through cardiovascular auscultation. Med Biol Eng Comput 2002; 40: 339–343.
27. Axelson D, Bakken IJ, Susann-Gribbestad I, Ehrnholm B, Nilsen G, Aasly J. Applications of neural network analyses to in vivo 1H magnetic resonance spectroscopy of Parkinson's disease patients. J Magn Reson Imag 2002; 16: 13–20.
28. Porenta G. Dorffner G, Kundrat S, Petta P, Duit-Schedlmayer J, Sochor H. Automated interpretation of planar thallium-201-dipyridamole stress-redistribution scintigrams using artificial neural networks. J Nucl Med 1994; 35: 2041–2047.
29. Hart A, Wyatt J. Connectionist models in medicine: an investigation of their potential. In: Proceedings of AIME'89 (2nd European Conference on Artificial Inteligence in Medicine, London 1989): Lecture notes in medical informatics: Vol. XXXVIII. Heilderberg: Springer, 1989: 115–124.
30. Cholewinski W, Stefaniak B, Poniatowicz-Frasunek E, Tarkowska A. Long lasting effect of physical stress on the LVEF. Nucl Med Rev Cent East Eur 2003; 6: 41–44.